

Controlling the properties of InGaAs quantum dots by selective-area epitaxy

S. Mokkapati,^{a)} P. Lever, H. H. Tan, and C. Jagadish

Department of Electronic Materials Engineering, Research School of Physical Sciences and Engineering, The Australian National University, Canberra, ACT 0200, Australia

K. E. McBean and M. R. Phillips

Microstructural Analysis Unit, University of Technology, Sydney, NSW 2007, Australia

(Received 16 September 2004; accepted 13 January 2005; published online 8 March 2005)

Selective growth of InGaAs quantum dots on GaAs is reported. It is demonstrated that selective-area epitaxy can be used for in-plane bandgap energy control of quantum dots. Atomic force microscopy and cathodoluminescence are used for characterization of the selectively grown dots. Our results show that the composition, size, and uniformity of dots are determined by the dimensions of the mask used for patterning the substrate. Properties of dots can be selectively tuned by varying the mask dimensions. A single-step growth of a thin InGaAs quantum well and InGaAs quantum dots on the same wafer is demonstrated. By using a single-step growth, dots luminescing at different wavelengths, in the range 1150–1230 nm, in different parts of the same wafer are achieved.

© 2005 American Institute of Physics. [DOI: 10.1063/1.1875745]

Photonic integrated circuits (PICs) have advantages of better optical performance, compact size, and low optical losses over individual photonic devices coupled through fibers. Fabrication of PICs requires in-plane bandgap energy control of epitaxial layers. Conventionally, growth of epitaxial material for PICs involves patterning the substrate, epitaxial growth, etching away some of the epitaxial layers, and regrowth. This process is repeated for each additional bandgap region to be added and requires high precision in controlling the thickness of regrown epitaxial layers for accurate alignment of the two optical devices. Even with perfect alignment, mode mismatch at the butt joint causes losses due to scattering and backreflection. Selective area epitaxy (SAE) eliminates the butt-joint problem of the traditional approach. In SAE the semiconductor substrate is patterned using a dielectric layer. Epitaxial growth does not take place on the dielectric and the growth species present over the dielectric migrate toward the mask openings. Growth rate at any place on the substrate is determined by the dimensions of the dielectric mask around that region. Thus, the properties of the epitaxial layers can be selectively controlled by changing the local mask dimensions. SAE has been used for fabrication and integration of quantum well (QW) devices.^{1–5} Photonic devices with quantum dots in the active region are superior to their QW counterparts because of their temperature independent properties⁶ and lower threshold current densities.⁷ Several groups have demonstrated photonic devices with quantum dots in the active region^{8–14} and SAE has been used to selectively grow quantum dots.^{15–17} In this work, we study SAE as a technique for tuning the emission wavelength of quantum dots with potential for quantum dot photonic device integration.

The GaAs substrates used for the growth of epitaxial layers studied in this work were patterned with SiO₂ deposited by plasma enhanced chemical vapor deposition, using photolithography and wet chemical etching. Quantum dots were then grown on these prepatterned substrates. Fig. 1

shows the schematic of mask patterns used in this study. The SiO₂ stripe widths (W) varied between 5 and 70 μm, whereas the openings (O) varied between 2 and 50 μm.

In_{0.5}Ga_{0.5}As quantum dots on GaAs were chosen as the subject of this study. All the samples were grown in a low-pressure (100 mbar), horizontal flow metalorganic chemical vapor deposition reactor. First, a 100 nm buffer layer was grown at 650 °C. The growth temperature was then reduced to 550 °C for the dot growth. The temperature was then ramped to 650 °C during the growth of 200 nm thick GaAs cap layer. An uncapped layer of dots was then grown at 550 °C for characterization with atomic force microscopy (AFM). All the samples grown were characterized using AFM and cathodoluminescence (CL) measurements. Oxford Instruments MonoCL2 system installed on a Jeol 35C scanning electron microscope was used for obtaining the CL spectra. The samples were excited using a 13 kV electron beam and the luminescence signal was detected using a liquid nitrogen cooled Hamamatsu R5509-72 detector.

The growth parameters were optimized so that the two dimension–three dimension (2D–3D) transition can be selectively achieved only in specific regions of the substrate. Under optimized growth conditions, no deposition takes place on the SiO₂ stripes. The In and Ga species present vertically above and on the stripes move away from the stripes through

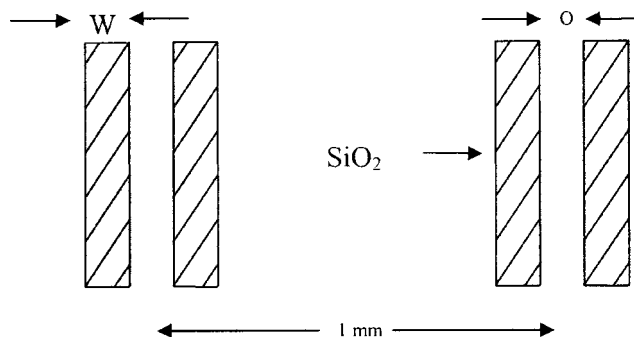


FIG. 1. Schematic showing the mask pattern used in this work.

^{a)}Electronic mail: smokkapati@ieee.org

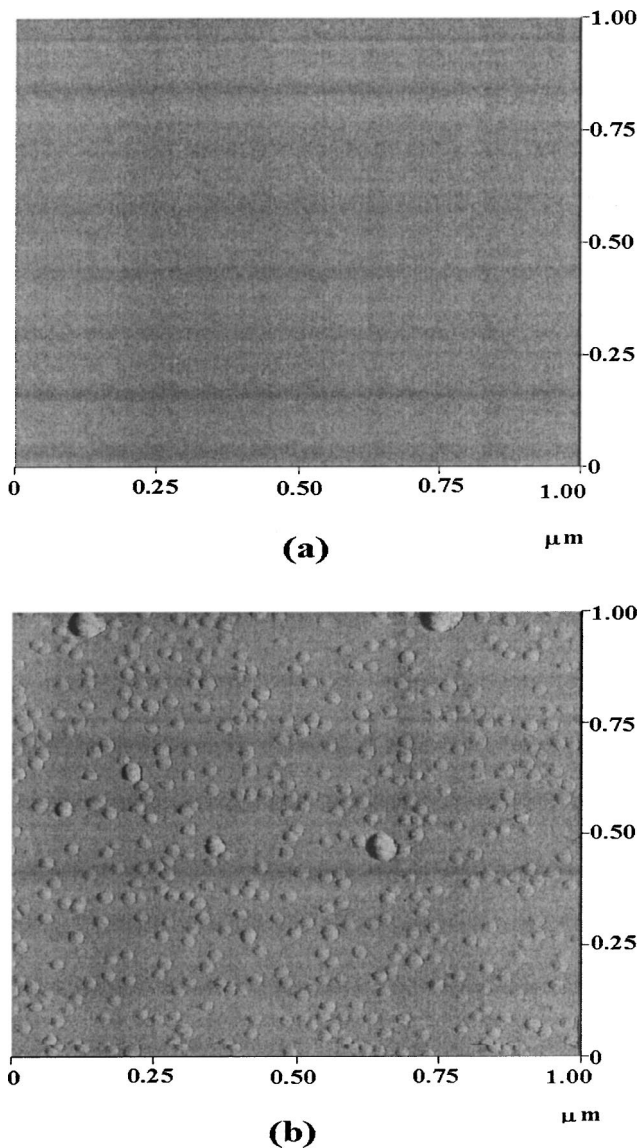


FIG. 2. AFM pictures ($1\ \mu\text{m} \times 1\ \mu\text{m}$) taken in different areas of the same wafer: (a) without silicon dioxide stripes and (b) between two silicon dioxide stripes of width (W) $15\ \mu\text{m}$, separated by $8\ \mu\text{m}$ openings (O).

surface migration and gas phase diffusion, causing enhanced deposition rates in regions adjacent to the stripes. The increase in deposition rate in the openings depends on their dimensions and the width of the dielectric mask. Thus, whether the 2D–3D transition takes place on the substrate or not depends on the dimensions of the mask surrounding that region. Figure 2 shows AFM pictures taken on different regions of the same substrate. $\text{In}_{0.5}\text{Ga}_{0.5}\text{As}$ was deposited for 2.0 s on the patterned semi-insulating (100)GaAs substrates. The rate of deposition was 1.7 monolayer (ML)/s, on an unpatterned substrate. In regions on the substrate where there are no SiO_2 stripes [Fig. 2(a)], the thickness of $\text{In}_{0.5}\text{Ga}_{0.5}\text{As}$ deposited is below the critical thickness of 4 ML for the 2D–3D transition, and we have a $\text{In}_{0.5}\text{Ga}_{0.5}\text{As}$ QW of thickness 3.4 ML. Due to the enhanced growth rate, we see quantum dots formed between stripes of width $15\ \mu\text{m}$ separated by $8\ \mu\text{m}$ [Fig. 2(b)]. As the emission peak of a QW is blue-shifted with respect to the emission peak from the quantum dots the QW region is transparent to the radiation emitted by the quantum dots. So the above proposed growth technique can be used in principle, to grow active material for fabrica-

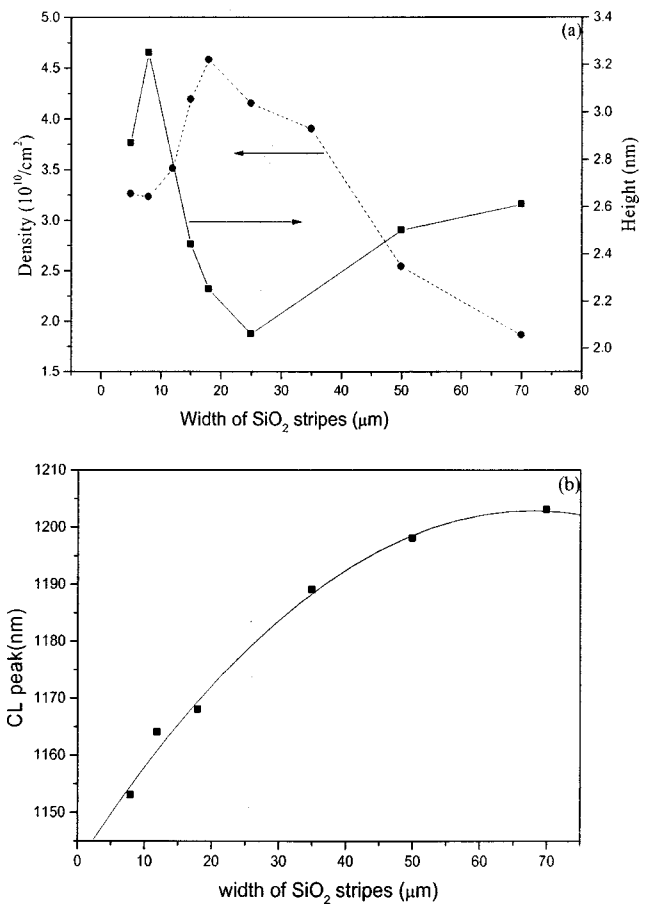


FIG. 3. Variation of (a) dot density and dot height and (b) peak emission wavelength as a function of stripe width, for a fixed opening of $50\ \mu\text{m}$.

tion of a quantum dot laser integrated with a passive waveguide or a modulator.

In the regions where dots are formed their properties can be tuned by varying the mask dimensions. Changing the SiO_2 stripe dimensions changes the growth rate or the total amount of material deposited, and hence enables us to control the physical and electronic properties of dots selectively. The growth parameters and mask dimensions were optimized for this study so that the total amount of material deposited is sufficient to cause the 2D–3D transition on all parts of the substrate. The deposition time was 3.0 s, at a rate of 1.7 ML/s on an unpatterned substrate. In our study we were able to vary the dot density between 3×10^{10} and $4.6 \times 10^{10}\ \text{cm}^{-2}$ without the creation of incoherent dots. The variation of dot size and dot density with mask dimensions is shown in Fig. 3(a). For an opening of $50\ \mu\text{m}$, as the stripe width is increased from 5 to $8\ \mu\text{m}$ the average dot height increases. However, with a further increase in the stripe width the dot density increases to a maximum of $4.6 \times 10^{10}\ \text{cm}^{-2}$, but accompanied by a simultaneous decrease in average dot height to a minimum of 2 nm. Further increase in stripe width causes formation of incoherent dots. The dot density no longer increases by increasing the stripe width once the defects start to appear. More and more material is drawn to these defects, as it is energetically favored, decreasing the dot density, and increasing the average dot height.

Figure 3(b) shows the variation of peak emission wavelength at 300 K from quantum dots as a function of the oxide stripe width for a fixed opening of $50\ \mu\text{m}$. The emission

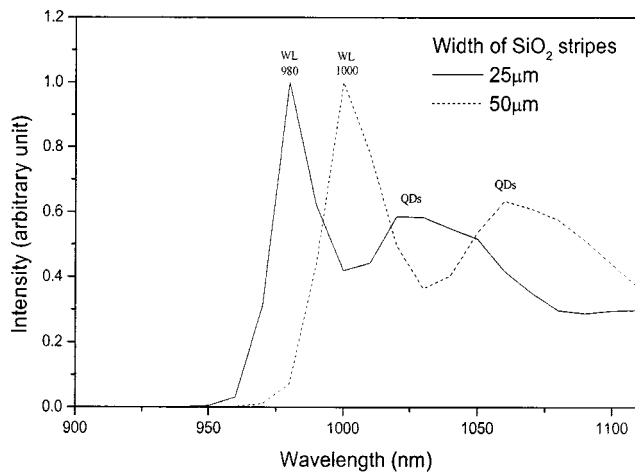


FIG. 4. CL spectra at 77 K from dots grown between SiO₂ stripes of widths 25 and 50 μm , separated by 50 μm .

wavelength first increases with increasing stripe width and then begins to saturate as the luminescence is quenched by the formation of incoherent dots. The ability to tune the emission wavelengths between 1150 and 1230 nm just by varying the mask dimensions was achieved. This growth scheme can be used in principle, to grow the active material for integrated multiple wavelength lasers for wavelength division multiplexing applications.

The emission wavelength of quantum dots depends on the size and composition of the dots. As the average dot size decreases the emitted radiation becomes shorter in wavelength. The decrease in average dot height from $W = 10\text{--}25\ \mu\text{m}$ [Fig. 3(a)] cannot be correlated to the increase in emission wavelength [Fig. 3(b)] with increasing stripe width. Figure 4 shows CL spectra from our dot samples at 77 K. The spectra show a sharp peak from the wetting layer (WL) and a broad peak from the dots. For a fixed opening of 50 μm , the WL peak redshifts from 980 to 1000 nm when the stripe width is increased from 25 to 50 μm . The shift in the WL peak shows that the wetting layer becomes more In rich as the width of the stripes is increased. This can be explained by taking into account the difference in mobilities of In and Ga adatoms. In adatoms are more mobile than the Ga adatoms, thereby causing the WL and the dots to become In rich. Thus, we conclude that the variation in emission wavelength of dots in this study is due to convolution of two

effects, namely the change in dot size and change in In content.

In summary, we studied the selective area growth of InGaAs quantum dots on patterned substrates and demonstrated that 2D–3D transition can be selectively achieved in certain regions of the substrate by optimizing the mask dimensions and growth conditions. This allows one to form quantum wells and quantum dots on different parts of the wafer in a single growth step. It was also demonstrated that one could tune selectively the size, density, composition, and emission wavelengths of the quantum dots. This is a promising technique which has great potential in realizing quantum dot based photonic integrated circuits.

Thanks are due to Michael Fraser, Kallista Stewart, Vince Craig, Manuela Buda, and Michael Aggett for fruitful discussions and expert advice. The Australian Research Council is gratefully acknowledged for the financial support.

- ¹R. M. Lammert, T. M. Cockerill, D. V. Forbes, and J. J. Coleman, *IEEE Photonics Technol. Lett.* **6**, 1167 (1994).
- ²M. L. Osowski, T. M. Cockerill, R. M. Lammert, D. V. Forbes, D. E. Ackley, and J. J. Coleman, *IEEE Photonics Technol. Lett.* **6**, 1289 (1994).
- ³R. M. Lammert, G. M. Smith, D. V. Forbes, M. L. Osowski, and J. J. Coleman, *Electron. Lett.* **31**, 1070 (1995).
- ⁴R. M. Lammert, G. M. Smith, J. S. Hughes, M. L. Osowski, A. M. Jones, and J. J. Coleman, *IEEE Photonics Technol. Lett.* **8**, 797 (1996).
- ⁵R. M. Lammert, S. D. Roh, J. S. Hughes, M. L. Osowski, and J. J. Coleman, *IEEE Photonics Technol. Lett.* **9**, 566 (1997).
- ⁶Y. Arakawa and H. Sakaki, *Appl. Phys. Lett.* **40**, 939 (1982).
- ⁷M. Asada, Y. Miyamoto, and Y. Suematsu, *IEEE J. Quantum Electron.* **QE-22**, 1915 (1986).
- ⁸H. C. Liu, M. Gao, J. McCaffrey, Z. R. Wasilewski, and S. Fafard, *Appl. Phys. Lett.* **78**, 79 (2001).
- ⁹A. D. Stiff-Roberts, S. Krishna, P. Bhattacharya, and S. Kennerly, *J. Vac. Sci. Technol. B* **20**, 1185 (2002).
- ¹⁰N. Kirstaedter, O. G. Schmidt, N. N. Ledentsov, D. Bimberg, V. M. Ustinov, A. Egorov, A. E. Zhukov, M. V. Maximov, P. S. Kopev, and Z. Alferov, *Appl. Phys. Lett.* **69**, 1226 (1996).
- ¹¹L. Harris, D. J. Mowbray, M. S. Skolnick, M. Hopkinson, and G. Hill, *Appl. Phys. Lett.* **73**, 969 (1998).
- ¹²K. Hinzer, C. N. Allen, J. Lapointe, D. Picard, Z. R. Wasilewski, S. Fafard, and A. J. SpringThorpe, *J. Vac. Sci. Technol. B* **18**, 578 (2000).
- ¹³N. Hatori, M. Sugawara, K. Mukai, Y. Nakata, and H. Ishikawa, *Appl. Phys. Lett.* **77**, 773 (2000).
- ¹⁴F. Heinrichsdofr, M. H. Mao, N. Kirstaedter, A. Krost, D. Bimberg, A. O. Kosogov, and P. Werner, *Appl. Phys. Lett.* **71**, 22 (1997).
- ¹⁵J. Tatebayashi, M. Nishioka, T. Someya, and Y. Arakawa, *Appl. Phys. Lett.* **77**, 3382 (2000).
- ¹⁶K. Kumakura, J. Motohisa, and T. Fukui, *J. Cryst. Growth* **170** (1997).
- ¹⁷T. S. Yeoh, R. B. Swint, A. Gaur, V. C. Elarde, and J. J. Coleman, *IEEE J. Sel. Top. Quantum Electron.* **8**, 833 (2002).